Flexible electron field emitters fabricated using conducting ultrananocrystalline diamond pyramidal microtips on polynorbornene films

K. J. Sankaran, N. H. Tai, and I. N. Lin

Citation: Applied Physics Letters **104**, 031601 (2014); doi: 10.1063/1.4862891

View online: http://dx.doi.org/10.1063/1.4862891

View Table of Contents: http://scitation.aip.org/content/aip/journal/apl/104/3?ver=pdfcov

Published by the AIP Publishing

Flexible electron field emitters fabricated using conducting ultrananocrystalline diamond pyramidal microtips on polynorbornene films

K. J. Sankaran,[1] N. H. Tai,[1,a)] and I. N. Lin[2,b)]
[1]*Department of Materials Science and Engineering, National Tsing-Hua University, Hsinchu 300, Taiwan*
[2]*Department of Physics, Tamkang University, Tamsui 251, Taiwan*

(Received 17 December 2013; accepted 8 January 2014; published online 21 January 2014)

High performance flexible field emitters made of aligned pyramidal shaped conducting ultrananocrystalline diamond (C-UNCD) microtips on polynorbornene substrates is demonstrated. Flexible C-UNCD pyramidal microtips show a low turn-on field of 1.80 V/μm with a field enhancement factor of 4580 and a high emission current density of 5.8 mA/cm^2 (at an applied field of 4.20 V/μm) with life-time stability of 210 min. Such an enhancement in the field emission is due to the presence of sp^2-graphitic sheath with a nanowire-like diamond core. This high performance flexible C-UNCD field emitter is potentially useful for the fabrication of diverse, flexible electronic devices. © *2014 AIP Publishing LLC*. [http://dx.doi.org/10.1063/1.4862891]

Science and technology of advanced materials can potentially modernize the society with flexible electronic devices such as wearable devices, distributed sensors, chip smart cards, electronic textiles, and various other basic components in different kinds of devices.[1,2] Various flexible electronic devices on such a potential substrate, based on thin films, nanoparticles, or the transfer of one dimensional (1D) nanostructures, such as paper displays,[3] light-emitting diodes,[4] field-effect transistors,[5] field emission displays (FEDs),[6] supercapacitors,[7] and heat spreaders[8] have already been realized. Besides the aforementioned applications FEDs on flexible substrates may actualize roll-up displays that are likely to impact everyone's daily life, particularly in terms of their fast response, low power consumption, and wide viewing angle.[9] Materials like semiconductor nanowires or nanotubes, carbon nanotubes, and diamond thin films have been reported to exhibit low turn-on voltages and high current densities, making them suitable for FEDs.[10,11] 1D nanostructures have received increasing attention due to their small tip radius and high aspect ratio, which exactly meet the requirements for good electron field emission (EFE) performance.[12–14] Among the likely materials, the unique physical and chemical properties, high thermal conductivity, and a surface with negative electron affinity make diamond a more promising material for FED devices.[15–17] The smaller grain size for diamond thin films[18] and the higher aspect ratio of sharpened tips[19] are the important ingredients required to improve the EFE properties. A special form of diamond, ultrananocrystalline diamond (UNCD) film, which possesses ultra-small grain sizes of 2–5 nm and very smooth film surfaces, has recently captured extensive interest because of its superb EFE behavior compared to that of micrometer-sized diamond films.[20–22] The grains in UNCD films consist of sp^3 carbon phases while the grain boundaries contain sp^2 carbon phases. The incorporation of N_2 in Ar/CH_4 plasma renders the UNCD films even more conductive, which enhances the electron transport and demonstrates a prominent potential for application of UNCD as an electron field emitter.[23–25] On the other hand, improvement of the field enhancement factor to amend EFE properties is a practice long been used. An effort to improve the EFE properties by making UNCD pyramidal tips grown in $CH_4/Ar/N_2$ medium has been reported.[26] Nevertheless, the integration of diamond nanostructures into flexible device architecture remains a technological challenge.

In this study, an efficient method of fabricating a flexible field emission device by incorporating arrays of pyramidal shaped conducting UNCD (C–UNCD) microtips onto a plastic substrate is demonstrated. Better EFE properties are accomplished and accounted.

A schematic description of the fabrication process is illustrated in Fig. 1. The SiO_2 coatings (1.2 μm thickness) on n-type silicon substrates were first patterned by the conventional photolithographic process to form SiO_2 pads (with different sizes of 2, 4, 6, 8 μm), followed by anisotropic etching of the Si materials using potassium hydroxide:normal propanol:deionized water solution to form inverted pyramidal microtips on Si substrates. The SiO_2 pads were then removed by buffered oxide etching, resulting in the inverted pyramidal Si microcavity array template [Fig. 1(a)]. Fig. 2(a) shows a field emission scanning electron microscopic image (FESEM; JEOL-6500) of typical inverted pyramidal shaped microcavities created on a Si substrate before the growth of the C-UNCD films. The inset of Fig. 2(a) shows the magnified FESEM image of a single inverted pyramidal microcavity, indicating that sharp inverted pyramidal shaped microcavities are created on the Si substrate. Four different sizes of inverted pyramidal shaped microcavities, ranging from 2 μm to 8 μm, were fabricated to facilitate a comparison.

The Si substrates containing these inverted pyramidal microcavities were then ultrasonicated in a methanol solution containing nanodiamond powders (~5 nm in diameter) and Ti powders (Sigma-Aldrich) (~325 mesh) for 45 min to facilitate the nucleation of C-UNCD films. C-UNCD films were deposited on the pre-seeded Si templates by the microwave plasma enhanced chemical vapor deposition (IPLAS, Cyrannus) system in a N_2 (94%)/CH_4 (6%) plasma with a

a)Electronic mail: nhtai@mx.nthu.edu.tw
b)Electronic mail: inanlin@mail.tku.edu.tw

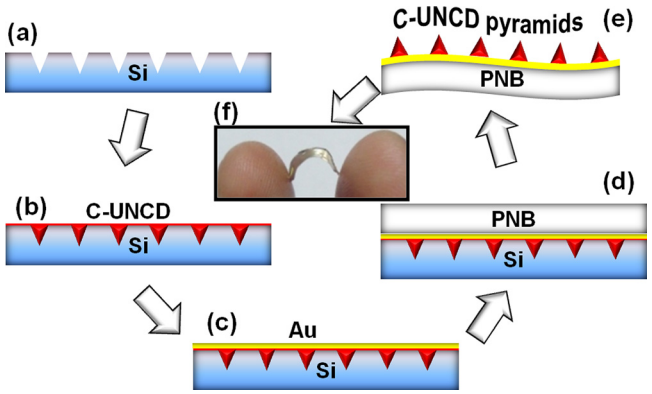

FIG. 1. Schematics of the process for fabricating flexible C-UNCD pyramidal microtips: (a) anisotropic etching of the Si substrates using potassium hydroxide:normal propanol:deionized water solution to form inverted pyramidal microcavities; (b) deposition of C-UNCD films on inverted pyramidal microcavities using the microwave plasma chemical vapor deposition system; (c) sputtered deposition of Cr (5 nm) and Au (100 nm) on C-UNCD films; (d) spin coating of PNB; (e) arrays of flexible C-UNCD pyramidal microtips after etching of Si; (f) the digital photograph of typical hand bent, flexible C-UNCD pyramidal microtips.

microwave power of 1200 W. The flow rate and the pressure were maintained at 100 sccm and 50 Torr, respectively. The substrate was heated to a temperature of 700 °C, which was monitored by a thermocouple embedded in the stainless steel substrate holder. Inverted pyramidal microcavity arrays

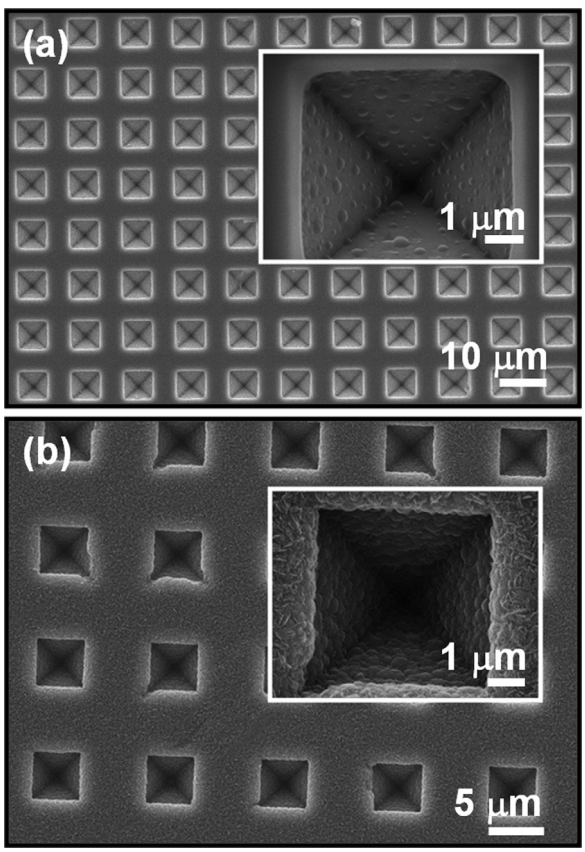

FIG. 2. FESEM image of (a) typical arrays of inverted pyramidal microcavities created on Si substrate with the inset showing the magnified FESEM images of a single inverted pyramidal microcavity and (b) the C-UNCD films coated inverted Si pyramidal microcavities with the inset showing the magnified FESEM images of a C-UNCD films coated single inverted pyramidal microcavity.

deposited with C-UNCD are shown in Fig. 2(b). This figure and the inset show evidence of very smooth and uniformly deposited C-UNCD films inside the inverted pyramidal microcavities. The conformal coating of the inverted pyramidal microcavities by C-UNCD films with the thickness about 750 nm is verified from this cross-sectional FESEM image (figure not shown).

The room temperature Hall measurements (ECOPIA HMS-3000) in the van der Pauw configuration taken on the C-UNCD films at millimeter scale reveals the negative value of the Hall coefficients, inferring that the majority of carriers in C-UNCD films are electrons. The carrier concentrations, mobility and electrical conductivity of the C-UNCD films are assessed to be about 1.0×10^{20} cm^{-3}, 11.6 cm^2 V^{-1} s^{-1}, and 186 S cm^{-1}, respectively. The conductivity of the C-UNCD films is comparable with the best conductivity obtainable for the UNCD films.[22,23,27]

A polynorbornene-based polymer (PNB; Avatrel 2585P) was chosen as the mechanically flexible base and the capping layer of the diamond-on-polymer devices due to its spin castability, flexibility, good adhesion to other materials, moisture inertness and resistance to acid.[28] After the deposition of C-UNCD films on inverted pyramidal Si microtips [Fig. 1(b)], a 1 μm thick PNB layer was spin coated onto C-UNCD films at a spin speed of 1500 rpm [Fig. 1(d)]. Prior to the spin coating of PNB, a 100 nm thick layer of Au was deposited on the C-UNCD films using a dc sputter deposition system (Helix) at a power of 50 W in argon partial pressure of 5 mTorr [Fig. 1(c)]. The Au layer serves to promote the formation of an ohmic contact to the C-UNCD pyramidal microtips. Notably, a thin layer of Cr (5 nm) was deposited before and after the Au coatings to achieve strong adhesion of Au with C-UNCD and PNB. After the spin coating process, the PNB coated C-UNCD substrates were baked at 100 °C (10 min), followed by annealing at 300 °C for 30 min. The backside etching of the substrates was carried out by using a solution of HF:HNO_3 (1:1) mixture to remove the Si completely by which the pyramidal shaped C-UNCD microtips were transferred to the PNB substrate. Upon release, the C-UNCD pyramidal microtips were effectively flipped over, as shown schematically shown in [Fig. 1(e)]. Figures 3(a)–3(d) show the FESEM images of the flexible C-UNCD pyramidal microtips with sizes of 2, 4, 6 and 8 μm, respectively. The digital photograph of hand-bent, flexible C-UNCD pyramidal microtips is shown in Fig. 1(f), indicating that the C-UNCD pyramidal microtips were capable of being flexed to a moderate radius of curvature (<5 mm) without causing delamination of the microtips from the polymer substrate.

The high magnification FESEM image [Fig. 4(a)] reveals the nanowire-like diamond grains with a length of 50–400 nm and a few nanometers in diameter for the C-UNCD films that are better illustrated by the transmission electron microscopy (TEM) image in Fig. 4(b). The nanowire-like diamond grains are highly dense and uniformly distributed in C-UNCD films. The selective area electron diffraction (SAED) pattern of the C-UNCD films [Fig. 4(c)] exhibits ring-shaped patterns, implying the random orientation of nanowire-like diamond grains in each of the small agglomerates of C-UNCD films. The SAED contains, besides the sharp diffraction rings corresponding to the

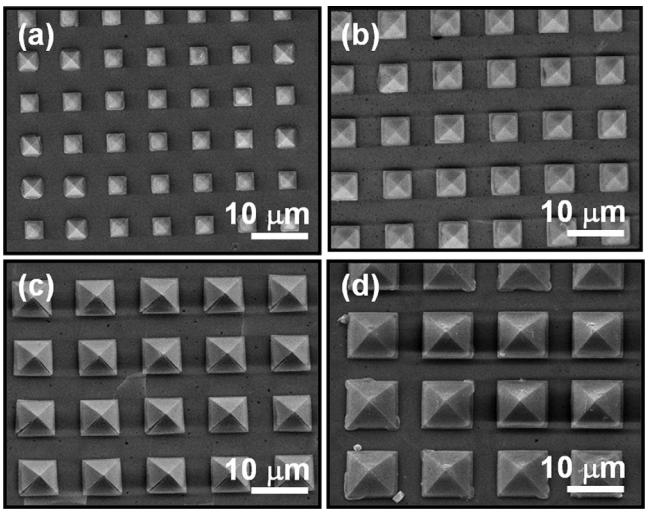

FIG. 3. FESEM images of fabricated flexible C-UNCD pyramidal microtips after the back side etching of silicon, with the tip size of (a) 2 μm, (b) 4 μm, (c) 6 μm, and (d) 8 μm.

lattice-plane of (311), (220), and (111) with the interplanar spacing estimated to be 0.11, 0.12, and 0.21 nm, respectively, a prominent diffused ring in the center, signifying the existence of graphitic (or amorphous carbon) phase in these films. The UV-Raman spectrum ($\lambda = 325$ nm; Lab Raman HR800, Jobon Yvon) of C-UNCD films [Fig. 4(d)] contains

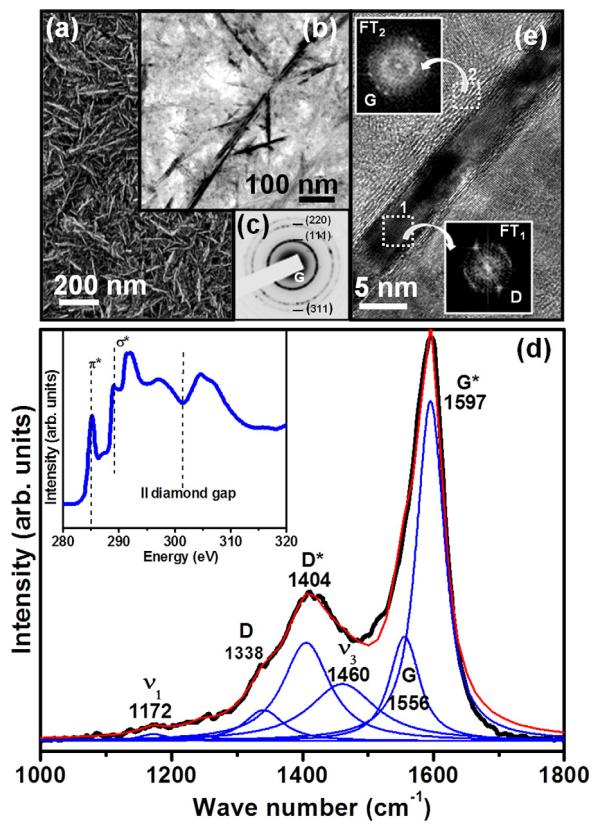

FIG. 4. (a) FESEM image of the C-UNCD films deposited on the pyramidal microtips. (b) The TEM micrograph of the typical region of the C-UNCD films with (c) the corresponding selective area electron diffraction (SAED) pattern. (d) UV-Raman spectrum and NEXAFS C-K edge spectrum (inset) of the C-UNCD films. (e) Typical HRTEM image of a single nanowire with its corresponding FT diffractogram displayed in the insets disclosing that the diamond grains FT_1 (area "1") are surrounded by graphitic phases FT_2 (area "2").

Raman peaks, which are characteristics of diamond materials with ultrasmall grain granular structure. There appears a resonance peak near 1338 cm^{-1} (D-band), which represents sp^3-bonds, indicating clearly the existence of diamond in the films. Moreover, there are ν_1-band and ν_3-band at 1172 cm^{-1} and 1460 cm^{-1}, representing the existence of *trans*-polyacetylene phase at grain boundaries[29] and D*-band at 1404 cm^{-1} and G-band near 1556 cm^{-1}, representing the presence of disordered carbons or nanographites. The inset of [Fig. 4(d)] shows a near-edge X-ray absorption fine structure (NEXAFS) C-K edge of C-UNCD films. Except for a typical sp^2-bonded carbon characteristic peak at 285.0 eV, NEXAFS of C-UNCD films is very similar to that of a single crystalline diamond. It exhibits one specific feature of a diamond exciton sharp peak at 289.0 eV and the other specific feature of a large dip at 302.5 eV which signifies a second absolute gap in the diamond band structure.[30–32] This confirms again the coexistence of sp^3 diamond and sp^2 graphitic phases in C-UNCD films that is line with the UV-Raman and TEM results.

The granular structure of the C-UNCD is unraveled by the high resolution TEM micrograph [Fig. 4(e)], exhibiting a clear core-shell microstructure. Each wire is found to be encased by the graphite phase. The thickness of the graphitic layer varies from a few atomic layers to more than 5 nm. The diamond and graphitic structures are confirmed by Fourier transformed (FT) diffractograms corresponding to the selected areas. The FT_1 pattern from the marked area "1" gives the ordering of the (111) planes of the diamond structure, whereas the FT_2 pattern from the marked area "2" points to the ordering of the (111) planes of the graphitic structure. These results confirm that each nanowire is diamond and is encapsulated by a sheath of graphitic phase. Consequently, the graphitic phases encasing the nanowires render the C-UNCD films highly conducting. The microstructural studies of C-UNCD films suggest that this graphitic content is formed during the growth of films. The abundance of the CN species in the N_2/CH_4 plasma may preferentially induce the growth of nanowire, along with the formation of graphitic phase encasing the nanowires, as the CN species invariably occupy the tip of the nanowire, promoting an anisotropic grain growth process.[25,33]

EFE properties of the flexible C-UNCD pyramidal microtips were measured using a tunable parallel plate setup, in which the cathode is C-UNCD pyramidal microtips and the anode is molybdenum rod with a diameter of 2 mm. The cathode-to-anode distance was controlled using a micrometer. The current-voltage (I-V) characteristics were measured using an electrometer (Keithley 2410) at pressure below 10^{-6} Torr. The emission current density versus applied field (J_e-E) curves were modeled using the Fowler-Nordheim (F-N) theory.[34] The turn-on field (E_0) value is designated as the applied field corresponding to J_e of 1.0 μA/cm^2. The EFE analysis results depicted in Fig. 5(a) demonstrate that these flexible C-UNCD pyramidal microtips are excellent field emitters, viz. possess low turn-on field (E_0) and high emission current density (J_e) values. The data presented in Fig. 5(a) are the average of EFE properties of flexible C-UNCD pyramidal microtips based EFE cathodic devices. The E_0 value is designated as the applied field corresponding to J_e of

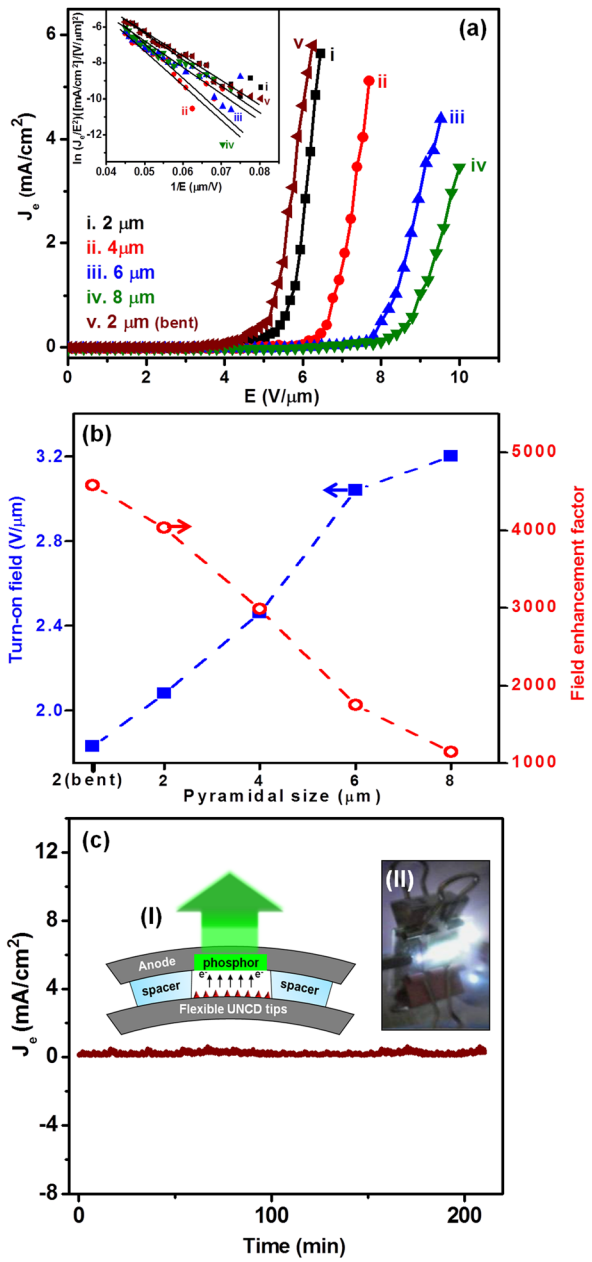

FIG. 5. (a) Electron field emission (EFE) current density (J_e) as a function of applied field (E) of different sizes of flexible C-UNCD pyramidal microtips (inset shows the corresponding Fowler-Nordheim plots, i.e., $\log(J_e/E^2)$-$1/E$ plots). (b) Variation in the turn-on field (E_0, solid squares) and field enhancement factor (β, open circles) of flexible C-UNCD pyramidal microtips with the sizes ranging from 2–8 μm and (c) the life-time stability measurement, i.e., the J_e versus time of the bent flexible C-UNCD 2 μm sized pyramidal microtips at $J_e = 0.2\,\text{mA/cm}^2$, where the inset "I" shows the schematic representation and the inset "II" shows the photograph image of the luminous field emission device with bent 2 μm sized C-UNCD pyramidal microtips as cathode.

1.0 μA/cm^2. The effect of tip size on the field emission behavior is evident from the results, viz. the E_0 value decreases consistently with the decrease of tip size [solid squares, Fig. 5(b)], with accompanying increase of the J_e value. A very low E_0 of 2.08 V/μm and a very high J_e of 5.5 mA/cm^2 (at an applied field of 4.25 V/μm) are achieved for the 2 μm sized pyramidal microtips.

Furthermore, the field enhancement factor (β) of the emission sites can be estimated from the F-N equation:[34] $J_e = (A\beta^2E^2/\varphi)\exp(-B\varphi^{3/2}/\beta E)$, where A and B are constants, ($A = 1.54 \times 10^{-6}\,\text{A eV V}^{-2}$ and $B = 6.83 \times 10^9\,\text{eV}^{-3/2}\,\text{V m}^{-1}$), E is the applied field, and φ is the work function of the emitting materials. From inset of Fig. 5(a), a plot of $ln\ (J_e/E^2)$ versus $(1/E)$, the F-N plot, gives a straight line. The actual β value can be estimated from the equation listed as follows: $\beta = [-6.8 \times 10^3\ \varphi^{3/2}]/m$, where m is the slope of the F-N plot. From the slopes of the F-N plots the β values for the arrays of different sized microtips were calculated by taking the φ value as 3.5 eV,[35,36] due to the fact that the nanowire-like diamond grains in the C-UNCD films contain a large amount of sp^2-bonded graphitic phases encasing the diamond grains that is evidenced from NEXAFS and TEM studies (cf., Fig. 4). The β values thus obtained are plotted in Fig. 5(b) as open circles. The observed 2 μm sized tips have excellent β value (4032) which is almost four times as much as that of the 8 μm sized tips (1145). Evidently, the large β value of the 2 μm sized pyramidal microtips is the reason for the enhancement of the EFE properties for the flexible emitters. These flexible C-UNCD pyramidal microtips exhibit far more efficient EFE properties than that of CNT based flexible field emitters.[37–40] How the unique granular structure of C-UNCD films, i.e., the nanowire-like diamond grains encased in a few layer graphitic phase, exhibit such a good EFE properties is not totally clear. The possible explanation is the nanoscale dielectric inhomogeneity proposed by Carey's and Ilie's groups.[41–43] They demonstrated that sp^2 clusters embedded in the sp^3 matrix or electronic disorder induced by localized defects oriented in the field direction can provide a local field enhancement to facilitate the emission. As a consequence, in the present C-UNCD films, conductive spatially localized sp^2-graphitic phase surrounding the wire-like sp^3-diamond grains, giving rise to dielectric inhomogeneities that lead to an enhanced local field at the tip as is indicated by the high β value.

Furthermore, we have performed the EFE measurements in bent configuration that is schematic represented in inset "I" of Fig. 5(c) for the flexible 2 μm sized C-UNCD pyramidal microtips. The J_e–E curve and the corresponding F-N plot are depicted in curve "v" and as inset "v" of Fig. 5(a), revealing the marvelous emission property of the bent flexible cathode with a radius of curvature of (<5 mm). The E_0 value decreases further to 1.80 V/μm and reaches a very high J_e of 5.8 mA/cm^2 (at an applied field of 4.20 V/μm) with high β value of 4580 for the bent 2 μm sized pyramidal microtips. The uniformity of the emission current from the bent 2 μm sized C-UNCD pyramidal microtips was confirmed from the luminescence of the phosphor coated on the anode plate. A luminescence image during field emission of bent 2 μm sized C-UNCD pyramidal tips at J_e of 0.2 mA/cm^2 is shown in the inset "II" of Fig. 5(c), revealing uniform emission pattern from the whole cathode area. I-V measurements were executed at several locations to confirm the uniformity of EFE characteristics. The examined EFE characteristics were independent of the locations, indicating nearly uniform fabrication over the whole substrate surface and resulting in a flexible robust cold cathode material. Interestingly, the bent 2 μm sized C-UNCD pyramidal microtips possess good life-time stability. The corresponding J_e versus time curve is shown as Fig. 5(c), indicating the emission current variations recorded over a period of 210 min at J_e of 0.2 mA/cm^2, which is the same J_e-level for

luminescence image [cf., inset II in Fig. 5(c)]. No significant discharges or spikes due to emitter adsorbates are produced and the emitted current remains constant over a period of time. The life-time stability measurement illustrates the other salient feature of the flexible C-UNCD pyramidal microtips, i.e., these emitters possess overwhelmingly superior emission reliably, compared with those made of CNT emitters.[37–40]

In summary, the present study provides an inexpensive fabrication approach towards a flexible EFE device based on the diamond pyramidal microtips that exhibits excellent field emission properties and is easily scalable. This simple method affords an approach for the application of pyramidal shaped C-UNCD microtips on plastic substrates. The effect of varying the sizes of the tips from 2 to 8 μm on the EFE properties is demonstrated. The 2 μm sized array of flexible C-UNCD pyramidal microtips in bent configuration reveal a very low E_0 value of 1.80 V/μm with high J_e value of 5.8 mA/cm^2 at an applied field of 4.20 V/μm. This flexible field emitting device exhibits a β value as large as 4580 and good emission current stability of 210 min. Such flexible C-UNCD pyramidal microtips can be potential candidates for an efficient field emitter material that opens a prospect for flat panel displays and high brightness electron sources.

The authors would like to thank the National Science Council, Taiwan, Republic of China, for the support of this research through the project No. NSC 102-2112-M-032-006-MY3 and NSC 101-2221-E-007-064-MY3.

[1]K. Nomura, H. Ohta, A. Takagi, T. Kamiya, M. Hirano, and H. Hosono, Nature **432**, 488 (2004).
[2]Y. He, W. Chen, C. Gao, J. Zhou, X. Li, and E. Xie, Nanoscale **5**, 8799 (2013).
[3]B. Comiskey, J. D. Albert, H. Yoshizawa, and J. Jacobson, Nature **394**, 253 (1998).
[4]A. Nadarajah, R. C. Word, J. Meiss, and R. Konenkamp, Nano Lett. **8**, 534 (2008).
[5]S. Park, M. Vosguerichian, and Z. Bao, Nanoscale **5**, 1727 (2013).
[6]H. J. Jeong, H. D. Jeong, H. Y. Kim, S. Y. Jeong, J. T. Han, and G. W. Lee, Small **9**, 2182 (2013).
[7]Y. Cheng, H. Zhang, S. Lu, C. V. Varanasi, and J. Liu, Nanoscale **5**, 1067 (2013).
[8]T. H. Kim, W. M. Choi, D. H. Kim, M. A. Meitl, E. Menard, H. Jiang, J. A. Carlisle, and J. A. Rogers, Adv. Mater. **20**, 2171–2176 (2008).
[9]Y. G. Sun and J. A. Rogers, Adv. Mater. **19**, 1897 (2007).
[10]L. Gangloff, E. Minoux, K. B. K. Teo, P. Vincent, V. T. Semet, V. T. Binh, M. H. Yang, I. Y. Y. Bu, R. G. Lacerda, G. Pirio, J. P. Schnell, D. Pribat, D. G. Hasko, G. A. J. Amaratunga, W. I. Milne, and P. Legagneux, Nano Lett. **4**, 1575 (2004).
[11]N. Shang, P. Papakonstantinou, P. Wang, A. Zakharov, U. Palnitkar, I. N. Lin, M. Chu, and A. Stamboulis, ACS Nano **3**, 1032 (2009).
[12]X. Wang, J. Zhou, C. Lao, J. Song, N. Xu, and Z. L. Wang, Adv. Mater. **19**, 1627 (2007).
[13]J. Liu, Z. Zhang, Y. Zhao, X. Su, S. Liu, and E. Wang, Small **1**, 310 (2005).
[14]Z. L. Wang, ACS Nano **2**, 1987 (2008).
[15]O. Shenderova, D. Brenner, and R. S. Ruoff, Nano Lett. **3**, 805 (2003).
[16]C. H. Hsu, S. G. Cloutier, S. Palefsky, and J. Xu, Nano Lett. **10**, 3272 (2010).
[17]H. Watanabe, C. E. Nebel, and S. Shikata, Science **324**, 1425 (2009).
[18]W. Zhu, G. P. Kochanski, and S. Jin, Science **282**, 1471 (1998).
[19]K. J. Sankaran, M. Afsal, S. C. Lou, H. C. Chen, C. Chen, C. Y. Lee, L. J. Chen, N. H. Tai, and I. N. Lin, Small **10**, 179 (2013).
[20]T. Chang, S. Lou, H. Chen, C. Chen, C. Lee, N. Tai, and I. Lin, Nanoscale **5**, 7467 (2013).
[21]K. J. Sankaran, K. Panda, B. Sundaravel, H. C. Chen, I. N. Lin, C. Y. Lee, and N. H. Tai, ACS Appl. Mater. Interfaces **4**, 4169 (2012).
[22]K. J. Sankaran, H. C. Chen, C. Y. Lee, N. H. Tai, and I. N. Lin, Appl. Phys. Lett. **101**, 241604 (2012).
[23]S. Bhattacharyya, O. Auciello, J. Birrell, J. A. Carlisle, L. A. Curtiss, A. N. Goyette, D. M. Gruen, A. R. Krauss, J. Schlueter, A. Sumant, and P. Zapol, Appl. Phys. Lett. **79**, 1441 (2001).
[24]K. J. Sankaran, Y. F. Lin, W. B. Jian, H. C. Chen, K. Panda, B. Sundaravel, C. L. Dong, N. H. Tai, and I. N. Lin, ACS Appl. Mater. Interfaces **5**, 1294 (2013).
[25]K. J. Sankaran, J. Kurian, H. C. Chen, C. L. Dong, C. Y. Lee, N. H. Tai, and I. N. Lin, J. Phys. D: Appl. Phys. **45**, 365303 (2012).
[26]P. T. Joseph, L. J. Chen, N. H. Tai, U. Palnitkar, H. F. Cheng, and I. N. Lin, J. Nanosci. Nanotechnol. **8**, 4198 (2008).
[27]J. P. Thomas, H. C. Chen, N. H. Tai, and I. N. Lin, ACS Appl. Mater. Interfaces **3**, 4007 (2011).
[28]R. A. Shick, S. K. Jayaraman, B. L. Goodall, L. F. Rhodes, W. C. McDougall, P. Kohl, S. A. Bidstrup-Allen, and P. Chiniwalla, Adv. Microelectron. **25**, 13 (1998).
[29]A. C. Ferrari and J. Robertson, Phys. Rev. B **63**, 121405 (2001).
[30]J. Birrell, J. E. Gerbi, O. Auciello, J. M. Gibson, D. M. Gruen, and J. A. Carlisle, J. Appl. Phys. **93**, 5606 (2003).
[31]Y. K. Chang, H. H. Hsieh, W. F. Pong, M. H. Tsai, F. Z. Chien, P. K. Tseng, L. C. Chen, T. Y. Wang, K. H. Chen, J. R. Bhusari, J. R. Yang, and S. T. Lin, Phys. Rev. Lett. **82**, 5377 (1999).
[32]P. T. Joseph, N. H. Tai, C. H. Chen, H. Niu, H. F. Cheng, W. F. Pong, and I. N. Lin, J. Phys. D: Appl. Phys. **42**, 105403 (2009).
[33]K. Teii and T. Ikeda, Diamond Relat. Mater. **16**, 753 (2007).
[34]R. H. Fowler and L. Nordheim, Proc. R. Soc. London, Ser. A. **119**, 173 (1928).
[35]J. B. Cui, J. Ristein, and L. Ley, Phys. Rev. B **60**, 16135 (1999).
[36]S. G. Wang, Q. Zhang, S. F. Yoon, J. Ahn, D. J. Yang, Q. Wang, Q. Zhou, and J. Q. Li, Diamond Relat. Mater. **12**, 8 (2003).
[37]H. S. Sim, S. P. Lau, H. Y. Yang, L. K. Ang, M. Tanemura, and K. Yamaguchi, Appl. Phys. Lett. **90**, 143103 (2007).
[38]M. Arif, K. Heo, B. Y. Lee, J. Lee, D. H. Seo, S. Seo, J. Jian, and S. Hong, Nanotechnology **22**, 355709 (2011).
[39]L. Yuan, Y. Tao, J. Chen, J. Dai, T. Song, M. Ruan, Z. Ma, L. Gong, K. Liu, X. Zhang, X. Hu, J. Zhou, and Z. L. Wang, Adv. Funct. Mater. **21**, 2150 (2011).
[40]V. P. Verma, S. Das, I. Lahiri, and W. Choi, Appl. Phys. Lett. **96**, 203108 (2010).
[41]J. D. Carey, R. D. Forrest, and S. R. P. Silva, Appl. Phys. Lett. **78**(16), 2339 (2001).
[42]A. Ilie, A. C. Ferrari, T. Yagi, S. E. Rodil, J. Robertson, E. Barborini, and P. Milani, J. Appl. Phys. **90**, 2024 (2001).
[43]A. Ilie, A. C. Ferrari, T. Yagi, and J. Robertson, Appl. Phys. Lett. **76**, 2627 (2000).